

Article

Effect of Peptide Length on *in Vitro* and *in Vivo* Properties of ^{177}Lu -labeled Peptide Analogs Targeting CCK2R

Anton Amadeus Hörmann^{1,*}, Maximilian Klingler¹, Christine Rangger¹, Christian Mair¹, Lieke Joosten², Gerben M. Franssen², Peter Laverman², Elisabeth von Guggenberg¹

1 Department of Nuclear Medicine, Medical University of Innsbruck, 6020 Innsbruck, Austria; anton.hoermann@i-med.ac.at (A.A.H.); klinglermaximilian@gmail.com (M.K.); christine.rangger@tirol-kliniken.at (C.R.); c.mair@tirol-kliniken.at (C.M.); elisabeth.von-guggenberg@i-med.ac.at (E.v.G.)

2 Department of Medical Imaging, Radboud University Medical Center, 6525 GA Nijmegen, The Netherlands; lieke.claessens-joosten@radboudumc.nl (L.J.); gerben.franssen@radboudumc.nl (G.M.F.); peter.laverman@radboudumc.nl (P.L.)

* Corresponding Author: anton.hoermann@i-med.ac.at, Tel: +43-512-504-83751

Abstract:

Minigastrin (MG) analogs for therapy of CCK2R-expressing malignancies are limited by low stability *in vivo* or excessive accumulation in non-target organs. By modifying the C-terminal receptor-binding sequence, metabolization could be prevented and tumor targeting significantly improved. In this work, *N*-terminal changes of the peptide length were evaluated. Based on the amino acid sequence of DOTA-MGS5 (DOTA-DGlu-Ala-Tyr-Gly-Trp-(N-Me)Nle-Asp-1Nal-NH₂), two new MG analogs were synthesized, by either introduction of a penta-DGlu moiety or depletion of the four *N*-terminal amino acids and introduction of a non-charged hydrophilic linker. Two CCK2R-expressing cell lines were used to demonstrate receptor interaction. Stability of the ^{177}Lu -labeled peptide analogs was evaluated in human serum up to 24 h after incubation and in BALB/c mice up to 30 min after injection. The biodistribution profile and tumor targeting potential was evaluated in xenografted BALB/c nude mice. For both new MG analogs, the combination of strong receptor-specific cell interaction, high stability and enhanced tumor targeting could be demonstrated. Shortening of the peptide sequence lowered the absorption in the dose-limiting organs, whereas elongation increased uptake in renal tissue.

Keywords: Cholecystokinin-2 receptor; minigastrin; peptide receptor radionuclide therapy; lutetium-177, theranostics

1. Introduction

The importance of radiolabeled peptides used in therapeutic intervention and diagnosis of tumor malignancies is rapidly increasing in modern medicine. These radiopeptides specifically recognize and bind to specific receptors on the cell surface. The cholecystokinin-receptor subtype 2 (CCK2R) is a G protein-coupled receptor physiologically located in the brain and gastrointestinal tract, mediating anxious behavior and gastric acid secretion in the stomach [1]. However, this receptor is overexpressed by several malignant tumors e.g., medullary thyroid carcinoma (MTC), small cell lung cancers, astrocytomas, stromal ovarian cancer, gastrointestinal stromal tumors, leiomyosarcomas, as well as selected gastrointestinal neuroendocrine tumors, breast and endometrial adenocarcinomas [2,3]. Different attempts have been made in the past to develop radiolabeled peptides derived from the natural ligands gastrin and cholecystokinin to selectively target the receptor for theranostic use [4–7]. The use of radiopeptides in peptide receptor radionuclide therapy (PRRT) is coupled to several prerequisites such as sufficient *in vivo* stability, high accumulation in tumor tissue with

concomitant low uptake in non-specific tissue, and predominant excretion via the renal system [8]. Early development of radioiodinated gastrin analogs demonstrated the feasibility of CCK2R targeting for therapeutic applications [9]. Therapeutic isotopes based on radiometals were introduced soon thereafter. The straightforward complexation chemistry based on bifunctional chelators, simplified the preparation of the radiopeptides for clinical use. Minigastrin (MG, Leu-(Glu)₅-Ala-Tyr-Gly-Trp-Met-Asp-Phe-NH₂), a member of the gastrin peptide hormone family, shares the C-terminal binding sequence "Trp-Met-Asp-Phe-NH₂", which is critical for receptor affinity [1,10,11]. This amino acid sequence was conjugated to the acyclic chelator diethylenetriaminepentaacetic acid (DTPA). In addition, leucine in position 1 was replaced by D-glutamic acid to improve the thermodynamic stability and kinetic inertness of the complex [12]. DTPA-DGlu¹-minigastrin (DTPA-MG0, DTPA-DGlu-(Glu)₅-Ala-Tyr-Gly-Trp-Met-Asp-Phe-NH₂) could be stably radiolabeled with β -minus emitting particles or γ -emitting radionuclides such as yttrium-90 or indium-111 [12,13]. Nevertheless, therapeutic implementation in the clinic was rather limited, since a major drawback being the high renal uptake caused unwanted side effects [14]. The penta-Glu moiety was linked to enhanced renal absorption; nevertheless, this moiety has also a significant impact on *in vivo* stability. For the truncated MG analog conjugated to the macrocyclic chelator 1,4,7,10-tetraazacyclododecane-1,4,7,10-tetraacetic acid (DOTA-MG11, DOTA-DGlu-Ala-Tyr-Gly-Trp-Met-Asp-Phe-NH₂) an inferior enzymatic stability was observed [14–16]. In a multicenter study funded by the European Cooperation in Science and Technology (COST BM0607: Targeted Radionuclide Therapy), twelve novel peptide analogs comprising the introduction of natural/unnatural amino acids, cyclization, dimerization, mainly in the *N*-terminal part of the linear peptide, were investigated [4,5,7]. DOTA-PP-F11 (DOTA-(DGlu)₆-Ala-Tyr-Gly-Trp-Met-Asp-Phe-NH₂), in which the stereochemistry of the penta-Glu moiety was switched to the D-isomeric form, showed favorable biodistribution with low kidney retention in female BALB/c mice. However, the stability issues were not considerably improved [4]. Site-specific exchange of amino acids in the C-terminal receptor specific binding sequence led to new peptide analogs with high stability against metabolic digestion *in vivo*. By replacement of phenylalanine with 1-naphtylalanine (1Nal) as well as substitution of oxidation sensitive methionine for *N*-methylated norleucine ((*N*-Me)Nle), the new MG analog DOTA-MGS5 (DOTA-DGlu-Ala-Tyr-Gly-Trp-(*N*-Me)Nle-Asp-1Nal-NH₂) was developed. In comparison with previously developed MG analogs, this peptide derivative radiolabeled with various radiometals exhibited enhanced receptor-specific cellular internalization and high resistance to enzymatic degradation leading to superior tumor targeting properties *in vivo* [17].

For DOTA-MGS5 labeled with lutetium-177, 86% and 70% intact radiopeptide was detected in the blood of BALB/c mice 10 min and 1 h after intravenous injection, respectively [17]. Further introduction of proline in different positions close to the *N*-terminus did not further improve the stability *in vivo* [18]. In the attempt to investigate possible alternative stabilization strategies in this study, the effect of the peptide length on the *in vitro* and *in vivo* CCK2R-targeting properties was further evaluated. Based on [¹⁷⁷Lu]Lu-PP-F11N, which is currently investigated in clinical studies (ClinicalTrials.gov Identifier: NCT02088645), the amino acid sequence of DOTA-MGS5 was elongated by introducing a penta-DGlu moiety [19]. Using a combination of the amino acid sequence of pentagastrin (PG, BOC- β Ala-Trp-Met-Asp-Phe-NH₂) and C-terminal modifications of DOTA-MGS5, the peptide length was shortened. Two moieties of 4-amino-3-hydroxybutyric acid (GABOB) were used as a linker to introduce a spatial distance between the chelator and the amino acid sequence, as the direct conjugation of the chelator to the pharmacophore region of the peptide might affect the CCK2R affinity. Reduced receptor affinity was found for des-BOC-pentagastrin (β Ala-Trp-Met-Asp-Phe-NH₂) and CCK4 (Trp-Met-Asp-Phe-NH₂), radioiodinated using the Bolton-Hunter reagent [10]. Similar findings were obtained with CCK4 directly conjugated to a bifunctional chelator, whereas the introduction of β -alanine (β Ala) and 6-aminohexanoic acid (Ahx) linkers allowed to retain affinity [20,21]. The *in vitro* characteristics of the new ¹⁷⁷Lu-labeled

peptide analogs were investigated, with specific focus on the stability against enzymatic degradation. Receptor affinity of the peptide analogs as well as cell internalization of the radiolabeled conjugates was studied using A431 epidermoid carcinoma cells stably transfected to express the human CCK2R (A431-CCK2R) as well as AR42J rat pancreatic cells expressing rat CCK2R [22]. Metabolic studies in BALB/c mice were performed to confirm a high resistance of the radiolabeled peptides against metabolic degradation also *in vivo*. The biodistribution and tumor targeting properties were evaluated in A431-CCK2R xenografted BALB/c nude mice, including, dosimetry estimates for dose limiting organs.

2. Materials and Methods

Materials

All commercially obtained chemicals were of analytical grade and used without further purification. Non-carrier-added [¹⁷⁷Lu]LuCl₃ produced from highly enriched ytterbium-176 was purchased from Isotope Technologies (ITM, Garching, Germany). The A431-CCK2R as well as A431-mock cells transfected to stably express human CCK2R were kindly provided by Dr. Luigi Aloj [23]. AR42J rat pancreatic cells, physiologically expressing rat CCK2R were purchased from ECACC (Salisbury, UK). Both A431-cell lines were cultured in Dulbecco's Modified Eagle Medium (DMEM) and AR42J cells were cultured in Roswell Park Memorial Institute (RPMI) 1640 Medium. Cell culture media were supplemented with 10% (v/v) fetal bovine serum and 5 mL of a 100x penicillin-streptomycin-glutamine mixture at 37°C in a humidified 95% air/5% CO₂ atmosphere. The cells were harvested using trypsin/EDTA solution (Sigma-Aldrich, Steinheim, Germany). Media and supplements were purchased from Invitrogen Corporation (Lofer, Austria). The peptide DOTA-MGS5 was purchased from piCHEM (Raaba-Grambach, Austria).

Peptide synthesis

The new minigastrin analogs DOTA-[(N-Me)Nle¹¹,1Nal¹³]PP-F11N (**1**) and DOTA-[(GABOB)₂,desBOC,(N-Me)Nle³,1Nal⁵]-PG (**2**) were synthesized by standard solid phase peptide synthesis using 9-fluorenylmethoxycarbonyl (Fmoc)-protected amino acids as described previously [24]. The following protective groups were used to protect the amino acids' reactive side chains: tert-butyl ester for Asp and DGlu, tert-butyl ether for Tyr, and tert-butyloxycarbonyl (BOC) for Trp. For coupling tris(tert-butyl) protected DOTA, a 3-fold molar excess was used.

Purification was carried out using RP-HPLC on a GILSON UV/VIS-155D multi-wavelength UV detector, equipped with an Eurospher II 100 Å 5µm C18 column, 250 x 8mm (Knauer, Berlin, Germany), combined with an Eurosil Bioselect 300 Å 5µm C18 precolumn, Vertex Plus A, 30 x 8 mm (Knauer, Berlin, Germany), using a water/0.1% TFA (A) and acetonitrile/0.1% TFA (B) gradient with a flow rate 2 mL/min: 0–4 min 20% B, 4–24 min 20–60% B, 24–26 min 60% B, 26–27 min 60–80% B, 27–28 min 80% B, 28–29 min 80–20% B, 29–37 min 20% B. The synthesized peptide conjugates with confirmed purity were characterized by MALDI-TOF MS (Bruker Microflex®, Bruker Daltonics, Bremen, Germany) lyophilized and stored at -20 °C for further use. Peptides were dissolved in water containing 20% EtOH or PBS (~1 µg/mL).

Radiolabeling and Characterization in Vitro

Radiolabeling with lutetium-177 was carried out using ~10 µg of DOTA-conjugate, ~40-150 MBq of ≤150 µL [¹⁷⁷Lu]LuCl₃ solution and a >1.2-fold volume of a 0.4 M sodium acetate/0.24 M gentisic acid solution with pH 5, reaching a radioactivity concentration of 0.3-3 GBq/mL. The reaction solution was incubated in a low protein binding Eppendorf tube (Eppendorf AG, Hamburg, Germany) at 90 °C for 20 min. The radiochemical purity was analyzed using an UltiMate 3000 chromatography system consisting of a variable UV-

detector (UV-VIS at $\lambda=220$ nm), an HPLC pump, an autosampler, a radiodetector (GabiStar, Raytest, Straubenhardt, Germany), equipped with a Phenomenex Jupiter 4 μ m Proteo 90 \AA C12 column, 250 \times 4.6 mm (Phenomenex Ltd., Aschaffenburg, Germany) with a flow rate of 1 mL and a water/acetonitrile/0.1% trifluoroacetic acid gradient with increasing concentrations of acetonitrile (ACN): 0–3 min, 10%; 3–18 min, 10%–55%; 18–20 min, 55%–80%; 20–21 min, 80%–10%; 20–25 min, 10%. Alternatively, an Agilent 1200 System (Agilent Technologies), with an in-line radiodetector (Elysia-Raytest, Liege, Belgium) equipped with a HiChrom C18 5 μ m, 4.6 \times 250 mm; column was used with a flow rate of 1 mL/min and a gradient with increasing concentrations of ACN: 0–5 min, 3%; 5–15 min, 3–100%; 15–25 min, 100%; 25–30 min, 100–3%; 30–35 min, 3%. The absence of radiocolloid formation was confirmed by iTLC-SG with 1 M ammonium acetate and methanol (1/1, *v/v*) as mobile phase.

For biodistribution experiments, the reaction solution was purified by solid phase extraction (SPE). For this purpose, a SepPak® tLight C18 cartridge (Waters, Milford, MA) was pre-treated with 5 mL 99% ethanol followed by 5 mL water. The reaction solution was passed through the cartridge and washed with 5 mL water to elute hydrophilic impurities. Elution of the radiolabeled peptides was performed using 0.7 mL of ethanol and 2.3 mL PBS. The solution for injection was prepared by dilution with PBS containing 0.5% BSA to avoid sticking to plastic material. The final bolus injection contained 20 pmol of total peptide in 150–200 μ L with less than 3% EtOH.

The stability studies with the ^{177}Lu -labeled peptide analogs were carried out at a concentration of 0.5 nmol peptide/mL in fresh human serum (*n*=2) for up to 24 h. A mixture of 0.1 nmol/mL of the radiolabeled peptides in PBS and octanol (1/1, *v/v*) was used to evaluate the octanol/PBS distribution coefficient ($\log D_{7.4}$; *n*=8). To determine the protein binding by Sephadex G-50 size-exclusion chromatography (GE Healthcare Illustra, Little Chalfont, UK), a 25 μ L serum sample was used for different time points after incubation. All steps were performed according to previously published protocols [24].

Cell Uptake and Receptor Binding Studies

Internalization experiments were performed in A431-CCK2R and AR42J cells. Non-specific uptake was assessed in A431-mock cells and by receptor blocking with 1 μ M pentagastrin for AR42J cells. The cells were seeded at a density of 1.0×10^6 for A431-CCK2R and 1.5×10^6 per well for the AR42J cells in 6-well plates (Greiner Labortechnik, Kremsmünster, Austria) and grown to confluence for 48 h. The cells were incubated with the different radiopeptides (final peptide concentration of 0.4 nM) at 37°C for up to 4 h, and the radioactivity of the lysed cells was determined in relation to the total radioactivity added (% internalized radioactivity). The specific cell uptake was determined by subtracting the uptake found in A431-mock cells from A431-CCK2 cells. For AR42J cells the uptake from blocking studies with pentagastrin (1000 nM) was used for subtraction.

The binding affinity of the new peptide analogs derived from DOTA-MGS5 for CCK2R was tested in a competition assay against [Leu^{15}]gastrin-I radiolabeled with iodine-125 and compared with pentagastrin (*n*=3). Radioiodination of [Leu^{15}]gastrin-I was carried out using the chloramine-T method as described previously [18]. Non-carrier-added [^{125}I][3-iodo-Tyr 12 ,Leu 15]gastrin-I was obtained by HPLC purification and stored in aliquots at -25°C. Binding assays were carried out in 96-well filter plates (MultiScreenHTS-FB, Merck Group, Darmstadt, Germany) pretreated with 10 mM TRIS/139 mM NaCl pH 7.4 (2 \times 250 μ L). For the assay, 400,000 A431-CCK2R cells per well were prepared in 20 mM HEPES buffer pH 7.4 containing 10 mM MgCl₂, 14 μ M bacitracin and 0.5% BSA. The cells were incubated in triplicates with increasing concentrations of the peptide conjugates (0.0003–1000 nM) and [^{125}I][3-iodo-Tyr 12 ,Leu 15]gastrin-I (25,000 cpm) for 1h at RT. Pentagastrin was included as an internal standard. Incubation was interrupted by filtration of the medium and rapid rinsing with ice-cold 10 mM TRIS/139 mM NaCl pH 7.4 (2 \times 200 μ L). The filters were collected and counted in a γ -counter (2480 Wizard2 3", PerkinElmer Life Sciences and Analytical Sciences, formerly Wallac Oy, Turku, Finland).

Half-maximal inhibitory concentration (IC_{50}) values were calculated following nonlinear regression with Origin software (Microcal Origin 6.1, Northampton, MA). For graphical presentation, data of exemplary binding curves were normalized from 0 to 100.

In Vivo Stability

Metabolic and biodistribution studies were performed in accordance with the ethical standards of the institution and approved by the Austrian Ministry of Science (BMWFV-66.011/0075-WF/V/3b/2019). *In vivo* stability studies of $[^{177}\text{Lu}]\text{Lu-1}$ and $[^{177}\text{Lu}]\text{Lu-2}$ were carried out in 5-7-week-old female BALB/c mice (n=6). A higher radioactivity of ~37 MBq, corresponding to ~1 nmol total peptide, was administered into the mice intravenously through a lateral tail vein to increase the detectability of potential radiometabolites by radio-HPLC. The mice were euthanized by cervical dislocation after 10 (n=2) and 30 (n=1) min post injection and the urine and a venous blood sample were collected at the time of sacrifice. Liver and kidneys were dissected and homogenized in 20 mM HEPES buffer pH 7.3 (1:1) with an Ultra-Turrax T8 homogenizer (IKA-Werke, Staufen, Germany) for 1 min at RT. Before radio-HPLC analysis the samples of blood, kidney and liver homogenates were treated with ACN to precipitate proteins (1:1), centrifuged (2000 g, 2 min) and the supernatant was diluted with water (1:1). Urine was diluted 1:4 with water before injection.

Biodistribution and Tumor Uptake

Preliminary biodistribution studies of ^{177}Lu -labeled DOTA-MGS5, **1** and **2** at 4 h p.i. were carried out in female BALB/c nude mice (Charles River; n=18) injected subcutaneously with A431-CCK2R as well as A431-mock cells (2×10^6 in 200 μL DMEM medium for each cell line) in the right and left flank at an age of 6–8 weeks. After 7–11 days when visible tumor xenografts were formed, groups of 5 mice were injected intravenously via a lateral tail vein with ~0.5 MBq of radiolabeled peptide, corresponding to 20 pmol of peptide, in a total volume of 150 μL in PBS/0.5% BSA. Using an additional mouse per group, a blocking study was performed by co-injecting a 1000-fold excess of the respective peptide analog (20 nmol) together with the radiolabeled peptide. For quantification, a 1:1, 1:10 and 1:50 standard was prepared using aliquots of the injection solution mixed with PBS/0.5% BSA. Mice were euthanized by cervical dislocation after 4h post injection (p.i.). Subsequently a blood sample was collected, and different tissues were dissected. All samples as well as the rest body were weighed, and the activity measured in the γ -counter together with the standard. Results were expressed as percentage of injected activity per gram of tissue (%IA/g).

Based on these preliminary studies, $[^{177}\text{Lu}]\text{Lu-2}$ was selected for further biodistribution studies evaluating the tumor uptake and tissue distribution for up to 7d p.i. in female BALB/c nude mice inoculated with A431-CCK2 cells at an age of 8–10 weeks (n=20). $[^{177}\text{Lu}]\text{Lu-2}$ was injected intravenously via lateral tail vein with ~1 MBq of radiolabeled peptide, corresponding to 20 pmol of peptide, in a total volume of 200 μL in PBS/0.5% BSA. For quantification, a 1% standard was used. After the different time points of 1 h, 24 h, 3 days, and 7 days, animals were euthanized by CO_2/O_2 -asphyxiation and a blood sample was immediately drawn, and tissues of interest (spleen, pancreas, stomach, intestine, kidneys, liver, heart, lung, muscle, femur, A431-CCK2R tumor, A431-mock tumor) were dissected. All collected samples were weighed and measured in the γ -counter together with the standard. Results were expressed as percentage of injected activity per gram of tissue (%IA/g), and tumor-to-organ activity ratios were calculated for selected tissues. For dose-limiting organs, kidneys and stomach, dosimetry estimates were calculated using Olinda-EXM (version 2.2, Vanderbilt University) and standard weights for humans (male and female). For this purpose, the % IA/g determined in mice was extrapolated to humans using the following equation: % IA per organ in humans = ($\% \text{IA/g}$ in mice \times mass of mice (kg)) \times mass of human organ (g)) / (total body mass (kg)). Time scaling was additionally applied to account for the faster kinetics in mice versus

humans using the following equation: time in humans = time in mice \times [mass of human (kg)/mass of mice] $^{1/4}$ [25]. The uptake values in mice were decay corrected for the adopted time points.

3. Results

Peptide Synthesis

The MG analogs **1** and **2** were synthesized starting with 100 mg resin, 240 μ mol each Fmoc-protected amino acid and 140 μ mol DOTA-tris(*tert*-butyl ester) according to a synthesis protocol published previously [24]. The amino acid sequence was defined per synthesis protocol. After purification by RP-HPLC and characterization by MALDI-TOF MS, the peptides were obtained with a chemical purity of at least 95% in moderate yields. The amino acid sequences and analytical data of the new peptide analogs are shown in Figure 1 and in Table 1. UV-chromatograms and mass spectrometry spectra are available in the Supporting Information (Figure S1 and S2). DOTA-MGS5 was obtained from piCHEM with confirmed purity of more than 95%.

Table 1. Amino acid sequence and analytical data of DOTA-MGS5, **1** and **2**.

Peptide	Amino acid sequence	Purity	MW calc <i>m/z</i> [M + H] ⁺	MW found <i>m/z</i> [M + H] ⁺
1	DOTA-(DGl)-Ala-Tyr-Gly-Trp-(N-Me)Nle-Asp-1Nal-NH ₂	>95%	2095.13	2094.13
2	DOTA-(GABOB) ₂ - β Ala-Trp-(N-Me)Nle-Asp-1Nal-NH ₂	>95%	1302.43	1302.34

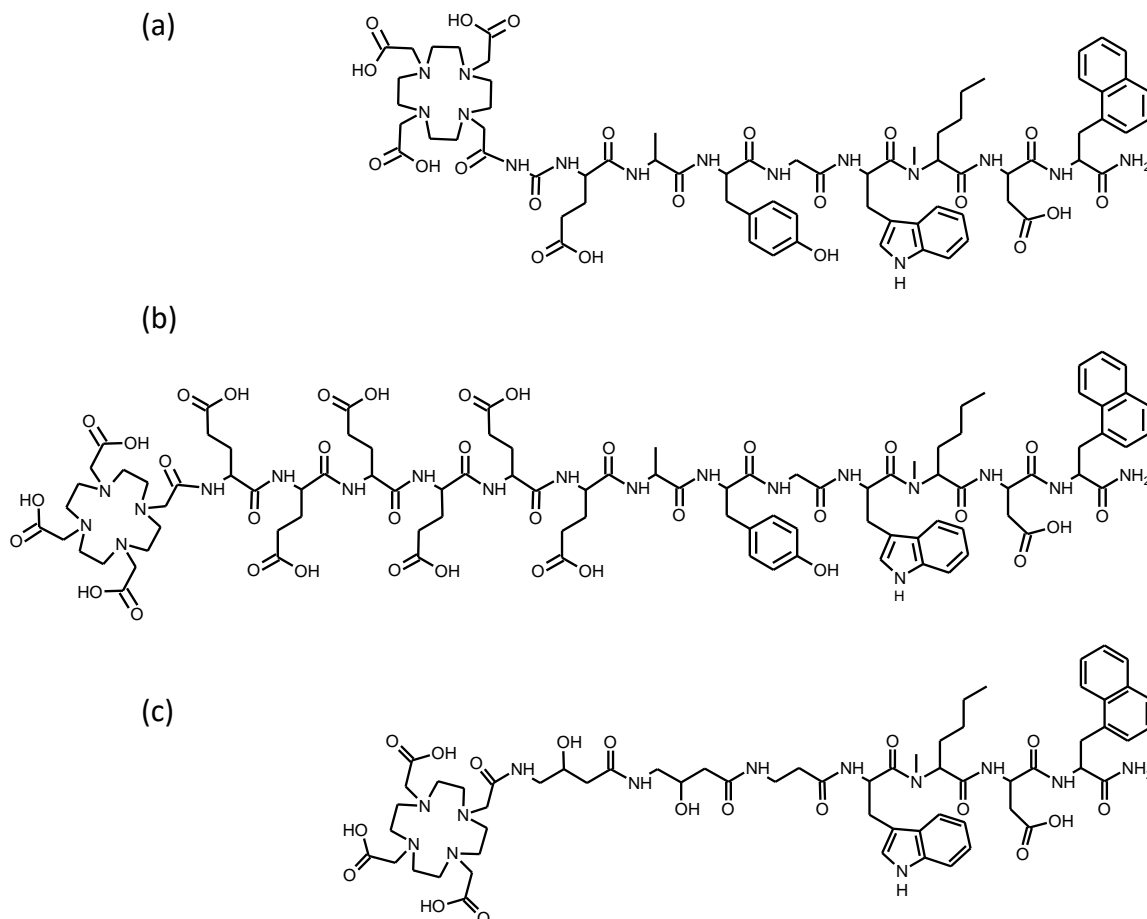


Figure 1. Chemical structure of (a) DOTA-MGS5, (b) **1** and (c) **2**

Radiolabeling and Characterization in Vitro

Radiolabeling with lutetium-177 using the described standard protocol resulted in a radiochemical purity of >95%. Radiocolloid formation was $\leq 1\%$. For *in vitro* assays, the radioligands were used without further purification. For biodistribution studies, an additional purification step by solid phase extraction as described above was used to remove any possible hydrophilic impurities. For metabolic studies with a higher injected radioactivity no purification was carried out, to avoid the intravenous injection of higher amounts of ethanol.

The new radiopeptides exhibited variable stability in fresh human serum. $[^{177}\text{Lu}]\text{Lu-1}$ showed a high stability after 24 h in serum, comparable to $[^{177}\text{Lu}]\text{Lu-DOTA-MGS5}$ ($97.2 \pm 0.1\%$ vs. $96.9 \pm 1.3\%$, respectively). For $[^{177}\text{Lu}]\text{Lu-2}$, a significantly lower stability with only $84.8 \pm 0.8\%$ intact radiopeptide observed after 24 h incubation ($p < 0.05$). The $\log D$ values in octanol/PBS showed highest hydrophilicity for $[^{177}\text{Lu}]\text{Lu-1}$ (-4.18 ± 0.24) followed by $[^{177}\text{Lu}]\text{Lu-DOTA-MGS5}$ (-2.25 ± 0.13) and $[^{177}\text{Lu}]\text{Lu-2}$ (-2.18 ± 0.38) with comparable values. Binding to human serum proteins was increased by a factor of two for $[^{177}\text{Lu}]\text{Lu-1}$ whereas $[^{177}\text{Lu}]\text{Lu-2}$ showed a decrease in protein binding of $\sim 50\%$ when compared to $[^{177}\text{Lu}]\text{Lu-DOTA-MGS5}$. The serum stability and protein binding over time is graphically shown in Figure 2 for all three radiopeptides.

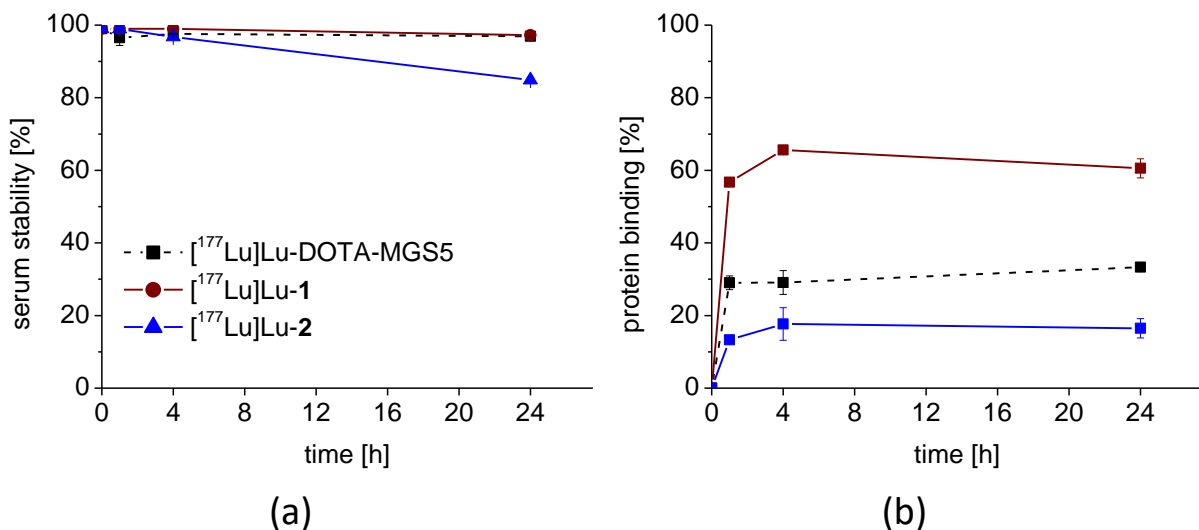


Figure 2. Serum stability (a) and protein binding (b) of the ^{177}Lu -labelled peptide analogs as determined by incubation in human serum at 37°C up to 24 h.

Cell Uptake and Receptor Binding Studies

For all ^{177}Lu -labeled peptide analogs, a high specific cell uptake was found for both CCK2R-expressing cell lines. $[^{177}\text{Lu}]\text{Lu-1}$ showed highest uptake in AR42J cells with uptake values of $65.5 \pm 1.6\%$ after 4h of incubation, whereas for $[^{177}\text{Lu}]\text{Lu-DOTA-MGS5}$ and $[^{177}\text{Lu}]\text{Lu-2}$ a somewhat lower uptake was observed at the same timepoint ($46.8 \pm 1.8\%$ and $41.4 \pm 2.7\%$). In A431-CCK2R cells, $[^{177}\text{Lu}]\text{Lu-1}$ showed even higher uptake values with $73.0 \pm 6.6\%$ after 4h after incubation, whereas for $[^{177}\text{Lu}]\text{Lu-DOTA-MGS5}$ and $[^{177}\text{Lu}]\text{Lu-2}$ uptake values of $66.2 \pm 4.3\%$ and $49.0 \pm 7.7\%$ were found, respectively. The non-specific uptake observed in blocking experiments using pentagastrin for AR42J cells as well as for A431-mock cells remained well below 1% for all ^{177}Lu -labeled peptide analogs at any timepoint studied. In Figure 3, the specific cell uptake of the three radiopeptides over time is shown for both cell lines ($n=3$ for each radiopeptide and cell line studied).

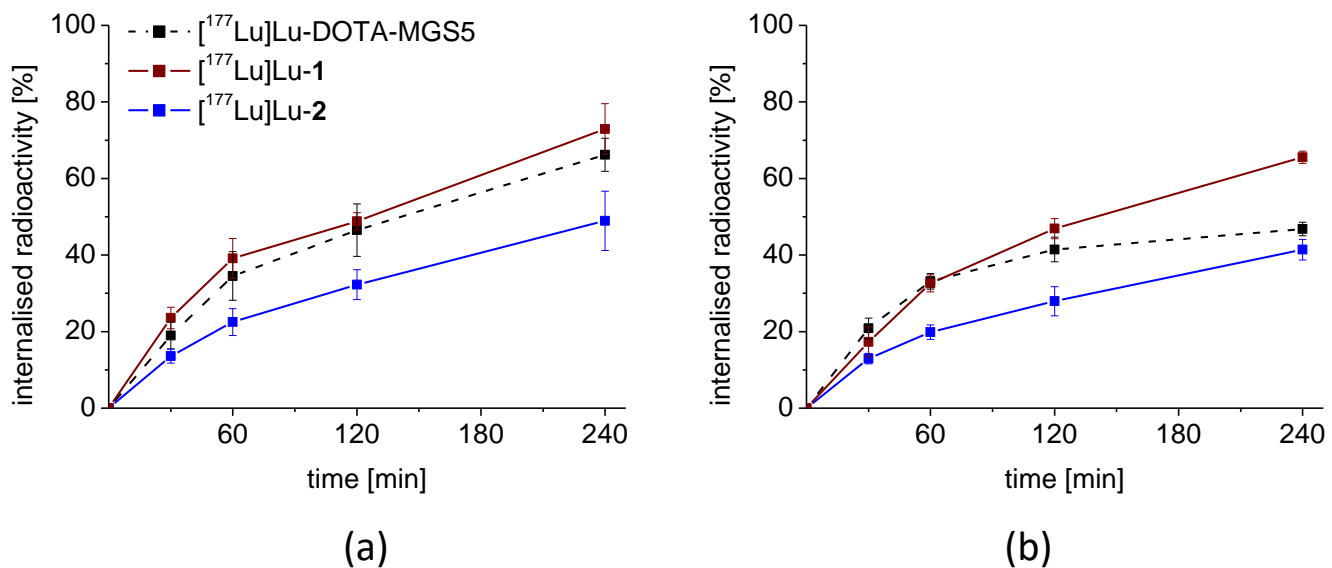


Figure 3. Specific cell uptake over time of $[^{177}\text{Lu}]\text{Lu-DOTA-MGS5}$, $[^{177}\text{Lu}]\text{Lu-1}$ and $[^{177}\text{Lu}]\text{Lu-2}$ in (a) A431-CCK2R cells and in (b) AR42J rat pancreatic cells for up to 4 h after incubation. Values are expressed as mean \pm SD from three independent experiments.

For both peptide analogs, a high affinity to the CCK2R comparable to pentagastrin was found. The lowest IC_{50} value of 0.18 ± 0.02 nM ($n=3$) was found for **1**. For **2**, a slightly higher IC_{50} value of 0.24 ± 0.8 nM ($n=3$) was calculated. However almost overlapping binding curves were observed for the two peptide analogs. Both peptide analogs demonstrated a higher affinity to the CCK2R compared to the reference peptide pentagastrin (0.84 ± 0.22 nM; $n=3$). Figure 4 shows exemplary normalized IC_{50} binding curves of **1** and **2** in comparison with pentagastrin. An IC_{50} value of 0.4 ± 0.2 was previously reported for DOTA-MGS5 [17].

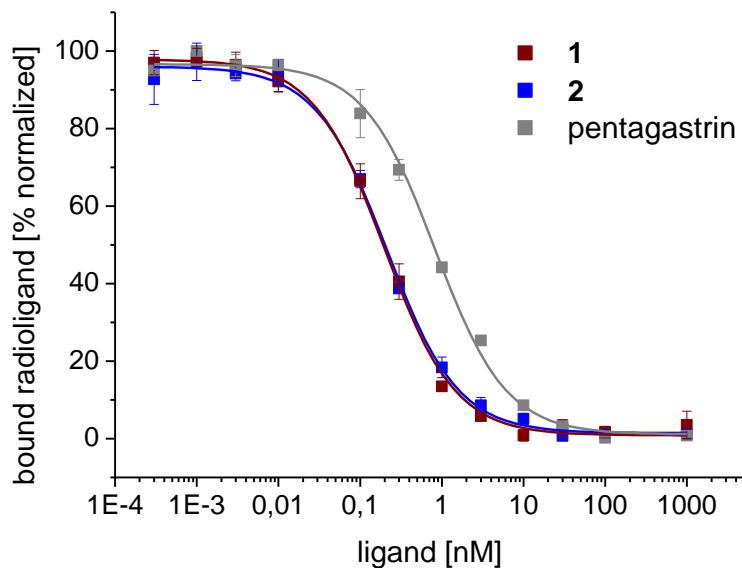


Figure 4. Exemplary normalized binding curves for **1**, **2** and pentagastrin in competition assays against $[\text{Leu}^{15}]\text{gastrin-I}$ radiolabeled with iodine-125 on A431-CCK2R cells.

In Vivo Stability and Biodistribution Studies

In the *in vivo* stability studies, a high resistance against enzymatic degradation could be observed for $[^{177}\text{Lu}]\text{Lu-2}$ when injected in BALB/c mice with more than $92.8\pm0.76\%$ and 84.4% intact radiopeptide in blood after 10 and 30 min after injection. A somewhat lower stability was found for $[^{177}\text{Lu}]\text{Lu-1}$ with values of $68.6\pm2.3\%$ and 44.0% for the same time points. Radiochromatograms of the blood samples at 10 min p.i. are displayed in Figure 5 in comparison with $[^{177}\text{Lu}]\text{Lu-DOTA-MGS5}$ (86% intact radiopeptide) previously studied [17]. More pronounced enzymatic breakdown was found in the urine samples, with highest amounts of intact radiopeptide found for $[^{177}\text{Lu}]\text{Lu-2}$ ($66.3\pm3.0\%$ and 60.2% after 10 and 30 min p.i., respectively). $[^{177}\text{Lu}]\text{Lu-1}$ showed a lower stability with only $42.4\pm9.7\%$ and 25.1% intact radiopeptide 10 and 30 min p.i., respectively. Also in kidney homogenates, a high rate of degradation was observed for $[^{177}\text{Lu}]\text{Lu-1}$ ($17.5\pm1.21\%$ and 3.9% for 10 and 30 min intact radiopeptide, respectively), whereas $[^{177}\text{Lu}]\text{Lu-2}$ demonstrated a much higher amount of intact radiopeptide ($59.7\pm2.9\%$ and 40.0% , 10 and 30 min p.i., respectively). In liver tissue homogenate samples, $87.1\pm18.27\%$ and 78.1% intact radiopeptide was found for $[^{177}\text{Lu}]\text{Lu-2}$, whereas $[^{177}\text{Lu}]\text{Lu-1}$ demonstrated only $54.9\pm5.6\%$ and 37.4% for the same timepoints.

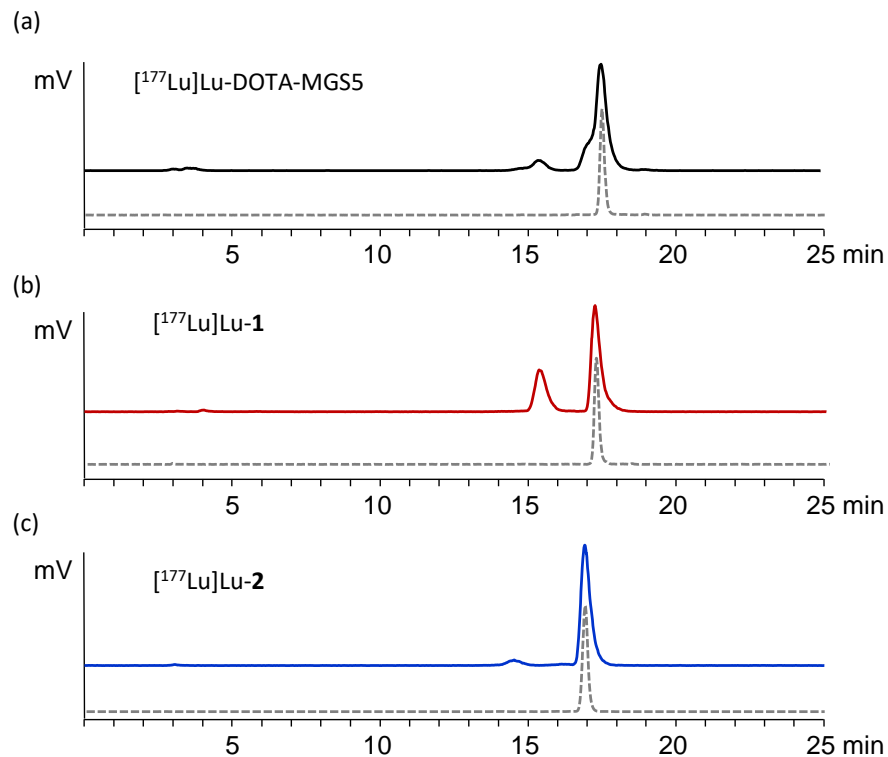


Figure 5. Radiochromatograms of the *in vivo* stability studies with (a) $[^{177}\text{Lu}]\text{Lu-DOTA-MGS5}$, (b) $[^{177}\text{Lu}]\text{Lu-1}$ and (c) $[^{177}\text{Lu}]\text{Lu-2}$ in BALB/c mice: colored lines showing analysis of blood samples 10 min p.i.; grey dotted line showing radiochromatogram after radiolabeling.

In the biodistribution studies performed at 4 h p.i., all three ^{177}Lu -labeled peptides showed a high accumulation of activity in A431-CCK2R xenografts with uptake values of $32.1\pm4.1\%$ IA/g for $[^{177}\text{Lu}]\text{Lu-2}$, $22.2\pm6.2\%$ IA/g for $[^{177}\text{Lu}]\text{Lu-1}$ and $22.9\pm4.7\%$ IA/g for $[^{177}\text{Lu}]\text{Lu-DOTA-MGS5}$. In A431-mock xenografts without CCK2R expression, a low non-specific tumor uptake below 1% IA/g was found for all radiopeptides. Tumor weight at the time of sacrifice was 301 ± 153 mg for A431-CCK2 and 217 ± 207 mg for A431-mock xenografts (n=24). In the blocking study performed with one single mouse for each radiopeptide, an effective inhibition of radioactivity accumulation in CCK2R-expressing tissue, with uptake values <1% IA/g in stomach, pancreas and A431-CCK2R-xenografts could be confirmed for all ^{177}Lu -labeled MG analogs. A very low non-specific tissue

uptake below 1% IA/g was observed also for blood, heart, lung, muscle and bone. Only the uptake of [¹⁷⁷Lu]Lu-DOTA-MGS5 in the liver was slightly higher (1.02±0.23% IA/g). [¹⁷⁷Lu]Lu-1 showed a considerably higher kidney uptake (21.6±2.11% IA/g), whereas the kidney uptake of [¹⁷⁷Lu]Lu-2 (1.96±0.29% IA/g) was reduced when compared to [¹⁷⁷Lu]Lu-DOTA-MGS5 (3.45±0.91% IA/g). In addition to that, the uptake of [¹⁷⁷Lu]Lu-1 in liver and spleen was also increased compared to both the other radiopeptides. In Figure 6, the uptake values found for A431-CCK2R xenografts and selected tissues (kidney, stomach, pancreas), including blocking, are graphically presented for all three radiopeptides. All other results from the biodistribution study are given in the Supporting Information (Table S1 and S2).

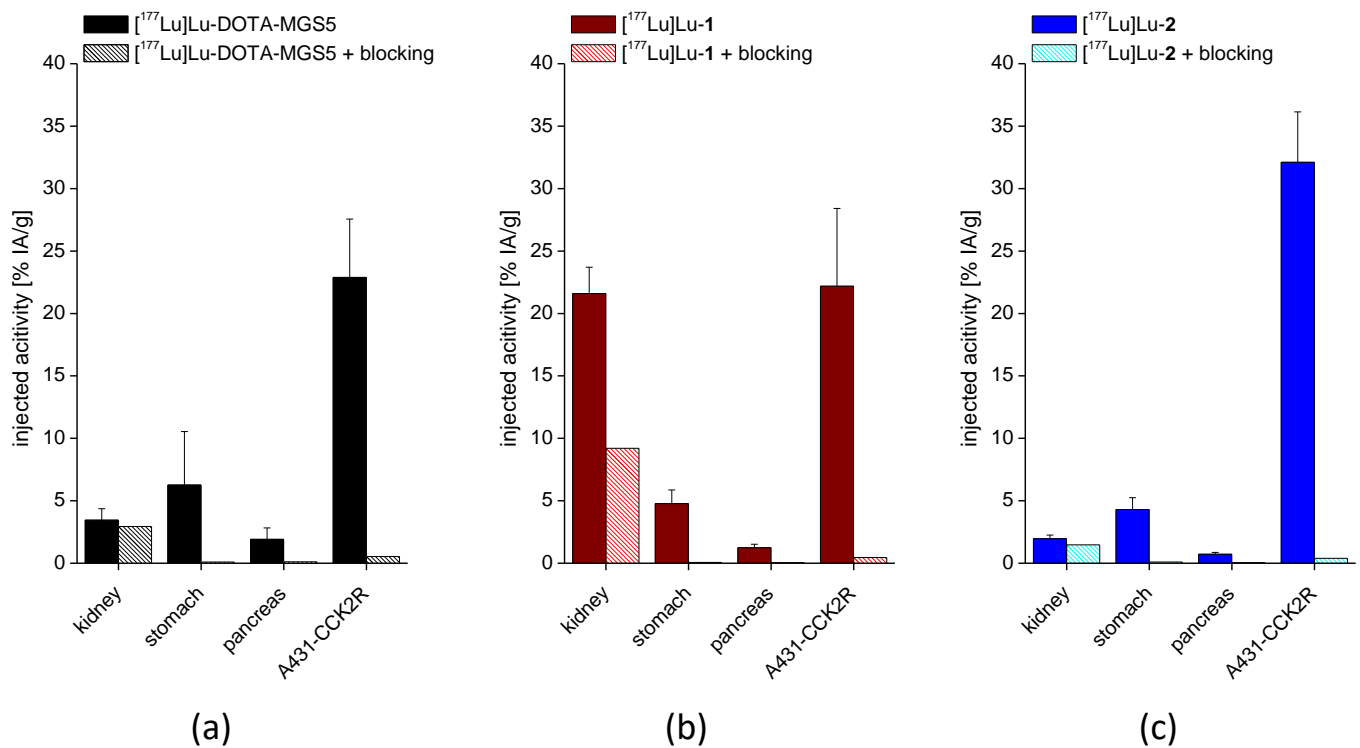


Figure 6. Biodistribution in selected organs of (a) [¹⁷⁷Lu]Lu-DOTA-MGS5, (b) [¹⁷⁷Lu]Lu-1 and (c) [¹⁷⁷Lu]Lu-2 in A431-CCK2 and A431-mock xenografted BALB/c nude mice at 4 h p.i., including blocking experiments using 1000-fold excess of non-radiolabeled peptide (n=18).

[¹⁷⁷Lu]Lu-2 showed lowest uptake in dose limiting organs, stomach and kidneys, while having the highest tumor accumulation. For this reason, this radiotracer was selected for an additional biodistribution study evaluating the tumor uptake and tissue distribution in A431-CCK2R xenografted BALB/c nude mice over up to seven days.

A rapid washout of the radioactivity from the blood pool was observed over time together with a low non-specific accumulation of radioactivity in most of the tissues. The uptake values in blood decreased from 1.45±0.30% at 1 h p.i. to 0.03±0.01% IA/g at 24 h p.i., and dropped to almost undetectable levels for the rest of the study. A low receptor specific uptake in stomach was confirmed with values of 5.43±1.05% IA/g at 1 h p.i. which was reduced by ~33% at 24 p.i. (3.66±0.38% IA/g) and slowly decreased to 2.28±0.33% and 0.88±0.12% IA/g after 3 and 7 days, respectively. A remarkable low uptake in kidneys already at 1 h p.i. with uptake values of only 2.84±0.42% IA/g was detected, which considerably decreased by ~54% after 24 h (1.32±0.23% IA/g) and further declined below 1% IA/g at 3 and 7 days after injection. The uptake in A431-CCK2R xenografts with values of 56.29±9.14% IA/g for the early time point of 1 h p.i. was considerably high, dropped by ~40% after 24 hours (33.61±2.95% IA/g) and continued to fall to levels of 12.52±0.96% IA/g

and $1.23 \pm 0.53\%$ IA/g 3 and 7 days after injection, respectively. Tumor weights, as determined at the time of sacrifice, were 174 ± 70 mg at 1 h p.i., 281 ± 66 mg at 24h, 440 ± 73 mg at 3 days and 380 ± 258 mg 7 days after injection.

In Figure 7, the washout over time for selected organs (A431-CCK2R xenograft, blood, kidney, stomach, and pancreas) is illustrated. Tumor-to-organ ratios for selected tissues (blood, stomach, and kidney) are shown in Table 2. In the Supporting Information, the distribution over time in the remaining tissues is given, together with the uptake values for all tissues analyzed (Figure S3 and Table S3).

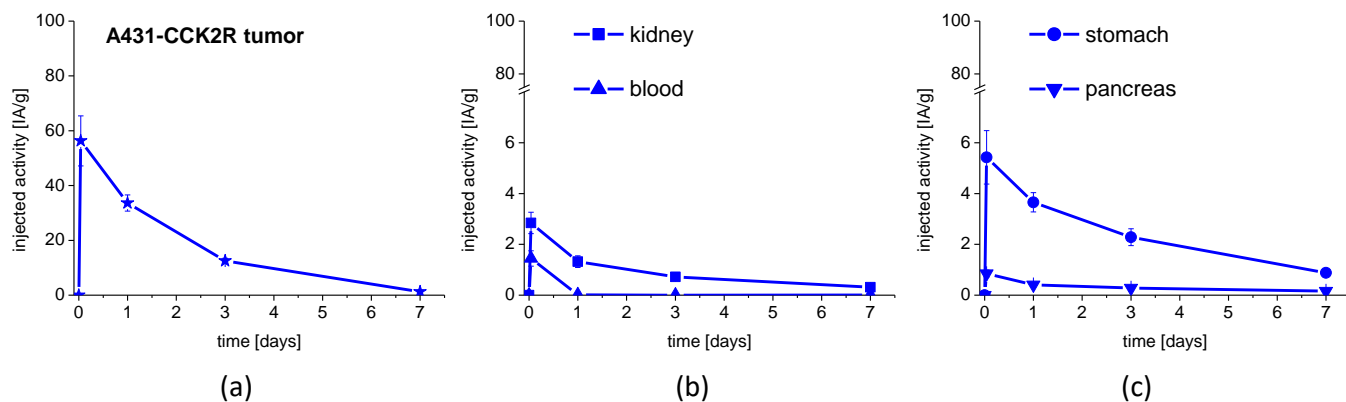


Figure 7. Uptake values of $[^{177}\text{Lu}]$ Lu-2 in (a) A431-CCK2R tumor xenograft, (b) blood and kidney and (c) stomach and pancreas for up to 7 days (n=5).

Table 2. Tumor-to-organ ratios of $[^{177}\text{Lu}]$ Lu-2 in A431-CCK2R xenografted BALB/c nude mice at 1 h, 24 h, 3 days and 7 days after injection.

Time point p.i.	1 h	24 h	3 days	7 days
Tumor-to-blood	38.9	3240.4	4856.5	241.2
Tumor-to-stomach	10.4	9.2	5.5	1.4
Tumor-to-kidney	19.8	25.5	17.3	4.0

Biodistribution data in A431-CCK2R xenografted BALB/c mice identified stomach and kidneys as the dose limiting organs for PRRT. Extrapolation of the % IA per organ in humans was based on the mean body weight of mice (18.1 g, n=20, range from 15.5-20.7 g) and the standard weights deduced from Olinda for men (body weight: 73.0 kg; stomach wall: 150 g, kidneys: 310 g) and women (body weight: 60.0 kg; stomach wall: 140 g, kidneys: 275.5 g). For time scaling a factor of 7.5-8.0 was calculated from the mean body weight of mice and set to 10. The calculated organ dose for stomach considering the wall as radiation source was 0.193 mGy/MBq for males and 0.2390 mGy/MBq for females. The calculated organ dose for kidneys was 0.0822 mGy/MBq for males and 0.0990 mGy/MBq for females.

4. Discussion

Using naturally occurring ligands with a high affinity for a particular target receptor as molecular templates is a common strategy in the development of radiotracers in nuclear medicine. Typically, peptide-based radiotracers are coupled to bifunctional chelators enabling for a simple and fast radiolabeling process with high yields of associated radiometals, making them effective for SPECT, PET, and targeted radiotherapy. Several approaches have been explored to overcome the low stability *in vivo* or excessive accumulation in non-specific organs of radiolabeled MG analogs targeting CCK2R [6,26-30]. In the past, no other modification within the receptor-binding sequence "Trp-Met-

Asp-Phe-NH₂” than substitution of Met with different amino acid analogs has been investigated to avoid a negative effect on the affinity. The MG analog with the sequence DOTA-DGlu-Ala-Tyr-Gly-Trp-(N-Me)Nle-Asp-1Nal-NH₂ (DOTA-MGS5) recently developed by our group showed favorable properties in terms of stabilization against metabolic degradation *in vivo* and enhanced tumor targeting. In this MG analog, site-specific modifications in the receptor-binding part of the linear peptide have been applied, by replacing Met with (N-Me)Nle, and Phe with 1Nal [17]. As introduction of additional substitutions in the linear peptide sequence did not lead to a further improvement in *in vivo* stability [18]. In this study we have investigated the possibility to change the peptide length. It has been previously shown, that the penta-DGlu sequence in DOTA-PP-F11N improved the overall stability *in vivo* resulting in enhanced tumor uptake [28]. The insertion of the penta-DGlu sequence in DOTA-MGS5 as evaluated for [¹⁷⁷Lu]Lu-1, resulted in higher hydrophilicity (-4.18±0.24), however increased protein binding (~60% after 24 h incubation) was observed in human serum. In [¹⁷⁷Lu]Lu-2, based on the sequence of pentagastrin, the peptide length of DOTA-MGS5 was shortened. Two moieties of GABOB were introduced as a linker, to improve the hydrophilic character of the conjugate. Previous studies with CCK4 derivatives confirmed the necessity to introduce a spacer, such as Ala or Ahx, between the bulky chelator and the receptor-binding sequence [20,21]. Furthermore a favorable impact on renal absorption and stability against enzymatic degradation was shown for non-charged amino acids, such as glutamine [30]. Even though similar logD values were observed for [¹⁷⁷Lu]Lu-2 and [¹⁷⁷Lu]Lu-DOTA-MGS5, the applied modifications led to a 2-fold decrease in serum protein binding (16.5±2.7% versus 33.3±0.9%, respectively). The observed differences in protein binding might have affected the results of the stability study in human serum, as contrasting results were observed in the metabolic study *in vivo*. It has been shown previously, that *in vitro* studies are not sufficient to predict the stability of MG analogs against metabolic degradation [31]. The changes in peptide length did not negatively affect the receptor affinity or cell internalization properties, which was confirmed using two different CCK2R-expressing cell lines. For all radiopeptides a low nanomolar affinity compared to the standard peptide pentagastrin was observed. A high specific cell uptake of 41-73% was confirmed for A431-CCK2R and AR42J cells at 4 h after incubation.

Most of the metabolic studies *in vivo* evaluating the stability of radiolabeled MG in the blood of mice have only been undertaken for short time periods of 5-10 min after injection. Given the improved stability of [¹⁷⁷Lu]Lu-DOTA-MGS5, in this study also a later timepoint of 30 minutes after injection was examined to get a better understanding of the stability of the novel MG analogs. Contrary to *in vitro* stability studies in human serum, [¹⁷⁷Lu]Lu-2 showed the highest *in vivo* stability with more than 84% intact radiopeptide after 30 min p.i. observed in the blood of BALB/c mice. A somewhat lower stability of 77% was observed for the lead structure [¹⁷⁷Lu]Lu-DOTA-MGS5 [17]. [¹⁷⁷Lu]Lu-1 showed the lowest *in vivo* stability with 44% intact radiopeptide detected in the blood of BALB/c mice at the same time point.

The high stabilization of [¹⁷⁷Lu]Lu-2 against enzymatic degradation was connected with improved tumor targeting, whereas the observed differences in *in vivo* stability of [¹⁷⁷Lu]Lu-1 and [¹⁷⁷Lu]Lu-DOTA-MGS5 did not impact the tumor targeting. Biodistribution studies were performed in A431-CCK2R and A431-mock xenografted BALB/c nude mice, allowing for a comparison with the results obtained for other CCK2R targeting peptide analogs. No human cell line with physiological CCK2R expression is currently available. In this study, a high uptake in A431-CCK2R xenografts of 22.9±4.7% IA/g was confirmed for [¹⁷⁷Lu]Lu-DOTA-MGS5 at 4 h after injection. With the two new MG analogs with different peptide length, a tumor uptake of 22.2±6.2% IA/g was observed for [¹⁷⁷Lu]Lu-1 and of 32.1±4.1% IA/g for [¹⁷⁷Lu]Lu-2. The uptake in A431-mock cells and the additional blocking experiment clearly confirmed the specificity of the CCK2R-mediated uptake. All three radiopeptides showed low accumulation in non-specific organs. However, the kidney uptake of [¹⁷⁷Lu]Lu-1 was ~6 times higher when compared to [¹⁷⁷Lu]Lu-DOTA-MGS5, confirming that the introduction of negatively charged *N*-

terminal amino acids affects the accumulation in renal tissue [30]. A much lower kidney uptake was observed for [¹⁷⁷Lu]Lu-2, which resulted to be decreased by a factor of ~2 in comparison with [¹⁷⁷Lu]Lu-DOTA-MGS5. Shortening of the amino acid sequence and introduction of a non-charged hydrophilic linker allowed for a considerable reduction in kidney uptake, resulting in a more than 2-fold improvement in tumor-to-kidney ratio (17 vs. 7, respectively).

For application in PRRT, increasing the radiation dosage that is given to the tumor cell while simultaneously decreasing the absorbed dose to non-specific tissue is of the utmost importance. When looking at the biodistribution profile of [¹⁷⁷Lu]Lu-2 over time, a high and persistent tumor uptake was achieved. A somewhat faster washout of the radioactivity from A431-CCK2R xenografts with values of ~56% versus ~13% IA/g at 1 h and 3 days after injection was observed as compared to CCK2R-expressing stomach. However, tumor-to-organ ratio at 3 days p.i. was still ~6 for stomach and ~17 for kidneys. Thus, with [¹⁷⁷Lu]Lu-2, showing a tumor uptake of >30% IA/g up to 24 h p.i., a 4-fold improvement in tumor uptake in comparison with [¹⁷⁷Lu]Lu-PP-F11N, currently under clinical investigation could be achieved [19,28]. The high tumor uptake of [¹⁷⁷Lu]Lu-2 combined with low accumulation in other tissues results in very favorable tumor-to-organ ratios, including also stomach and kidneys, which have been identified as dose limiting organs. Radiation-induced damage to the dose-limiting organs is reduced during PRRT by dividing the dosage into multiple cycles. By extrapolation of the absorbed dose in stomach wall and kidneys from mouse to humans and considering four consecutive treatments with 8 GBq of [¹⁷⁷Lu]Lu-1, a cumulative absorbed radiation dose of <10 and <5 Sv was estimated for stomach and kidneys, respectively. Thus it can be expected, that during PRRT the cumulative doses to stomach (50 Gy) and kidneys (27 Gy) will not be reached [32,33]. These values compare well to the previous published data on dosimetry calculations for PRRT with [¹⁷⁷Lu]Lu-PP-F11N in patients, anticipating a cumulative dose of <15 Sv for the stomach and <5 Sv for the kidneys after four cycles with 8 GBq [19].

5. Conclusions

In this study, two new ¹⁷⁷Lu-labeled MG analogs based on the sequence of DOTA-MGS5 by either introduction of a penta-DGlu moiety or depletion of the four N-terminal amino acids and introduction of GABOB-GABOB-βAla as a linker were synthesized and evaluated for their potential therapeutic use. The introduction of multiple negative charges into [¹⁷⁷Lu]Lu-1 clearly affected renal accumulation leading to a suboptimal biodistribution profile, whereas the combined use of the modified receptor-specific sequence “Trp-(N-Me)Nle-Asp-1Nal-NH₂” of DOTA-MGS5 and a non-charged hydrophilic linker in [¹⁷⁷Lu]Lu-2 led to a further enhancement in tumor uptake and favorable tumor-to-organ ratios, confirming the high potential of these new class of radiolabeled MG analogs for therapeutic use in CCK2R-expressing malignancies.

Supplementary Materials: Figure S1: UV-chromatogram of (a) DOTA-MGS5, (b) 1 and (c) 2; Figure S2: Mass spectra of (a) DOTA-MGS5, (b) 1 and (c) 2; Figure S3. Uptake of [¹⁷⁷Lu]Lu-2 in the residual organs of A431-CCK2 xenografted BALB/c nude mice for up to 7 days; Table S1: Results of biodistribution studies evaluated in A431-CCK2R/A431-mock xenografted BALB/c nude mice of the ¹⁷⁷Lu-labeled peptide derivatives (20 pmol, 4 h p.i.); Table S2. Results of the blocking experiments using 1000-fold excess of non-radiolabeled peptide in the biodistribution study evaluated in A431-CCK2R/A431-mock xenografted BALB/c nude mice of the ¹⁷⁷Lu-labeled peptide derivatives (20 pmol, 4 h p.i.); Table S3. Uptake values of [¹⁷⁷Lu]Lu-2 in A431-CCK2R tumor xenograft for up to 7 days.

Author Contributions: Conceptualization, supervision, project administration and funding acquisition, E.v.G.; methodology and investigation, A.A.H., M.K., C.R., C.M., L.J., G.M.F., P.L. and E.v.G.; writing—original draft preparation: A.A.H.; writing—review and editing, E.v.G., C.R., M.K., L.J., G.M.F., P.L.; All authors have read and agreed to the published version of the manuscript.

Funding: This study was financially supported by the Austrian Science Fund (FWF), project P 34732-B.

Informed Consent Statement: Not applicable.

Data Availability Statement: Data are contained within the article.

Acknowledgments: Eva Forer and Taraneh Zavvar are greatly acknowledged for technical assistance.

Conflicts of Interest: The Medical University of Innsbruck has filed a patent application for minigastrin analogues with "Improved pharmacokinetics and cholecystokinin-2 receptor (CCK2R) targeting for diagnosis and therapy".

1. Noble, F.; Wank, S.A.; Crawley, J.N.; Bradwejn, J.; Seroogy, K.B.; Hamon, M.; Roques, B.P. International Union of Pharmacology. XXI. Structure, Distribution, and Functions of Cholecystokinin Receptors. *Pharmacol Rev* **1999**, *51*, 745–781.
2. Reubi, J.C.; Targeting CCK receptors in human cancers. *Curr Top Med Chem* **2007**, *7*, 1239–1242.
3. Reubi, J.C.; Schaer, J.C.; Waser, B. Cholecystokinin(CCK)-A and CCK-B/Gastrin Receptors in Human Tumors. *Cancer Res* **1997**, *57*, 1377–1386.
4. Ocak, M.; Helbok, A.; Rangger, C.; Peitl, P.K.; Nock, B.A.; Morelli, G.; Eek, A.; Sosabowski, J.K.; Breeman, W.A.P.; Reubi, J.C.; et al. Comparison of Biological Stability and Metabolism of CCK2 Receptor Targeting Peptides, a Collaborative Project under COST BM0607. *Eur J Nucl Med Mol Imaging* **2011**, *38*, 1426–1435.
5. Aloj, L.; Aurilio, M.; Rinaldi, V.; D'ambrosio, L.; Tesauro, D.; Peitl, P.K.; Maina, T.; Mansi, R.; von Guggenberg, E.; Joosten, L.; et al. Comparison of the Binding and Internalization Properties of 12 DOTA-Coupled and ¹¹¹In-Labelled CCK2/Gastrin Receptor Binding Peptides: A Collaborative Project under COST Action BM0607. *Eur J Nucl Med Mol Imaging* **2011**, *38*, 1417–1425.
6. Roosenburg, S.; Laverman, P.; van Delft, F.L.; Boerman, O.C. Radiolabeled CCK/Gastrin Peptides for Imaging and Therapy of CCK2 Receptor-Expressing Tumors. *Amino Acids* **2011**, *41*, 1049–1058.
7. Laverman, P.; Joosten, L.; Eek, A.; Roosenburg, S.; Peitl, P.K.; Maina, T.; Mäcke, H.; Aloj, L.; von Guggenberg, E.; Sosabowski, J.K.; et al. Comparative Biodistribution of 12 ¹¹¹In-Labelled Gastrin/CCK2 Receptor-Targeting Peptides. *Eur J Nucl Med Mol Imaging* **2011**, *38*, 1410–1416.
8. Kaloudi, A.; Nock, B.A.; Krenning, E.P.; Maina, T.; Jong, M.D. Radiolabeled Gastrin/CCK Analogs in Tumor Diagnosis: Towards Higher Stability and Improved Tumor Targeting. *Tumor Target* **2015**, *59*, 18.
9. Reubi, J.C.; Waser, B. Unexpected High Incidence of Cholecystokinin-B/Gastrin Receptors in Human Medullary Thyroid Carcinomas. *Int. J. Cancer* **1996**, *67*, 644–647.
10. Behr, T.M.; Jenner, N.; Bă, M. Radiolabeled Peptides for Targeting Cholecystokinin-B/Gastrin Receptor-Expressing Tumors. *J Nucl Med* **1999**, *40*(6), 1029–1044.
11. Dufresne, M.; Seva, C.; Fourmy, D. Cholecystokinin and Gastrin Receptors. *Physiol Rev* **2006**, *86*, 43.
12. Béhé, M.; Becker, W.; Gotthardt, M.; Angerstein, C.; Behr, T.M. Improved Kinetic Stability of DTPA-DGlu as Compared with Conventional Monofunctional DTPA in Chelating Indium and Yttrium: Preclinical and Initial Clinical Evaluation of Radiometal Labelled Minigastrin Derivatives. *Eur J Nucl Med Mol Imaging* **2003**, *30*, 1140–1146.
13. Behr, T.M.; Béhé, M. Cholecystokinin-B/Gastrin Receptor-Targeting Peptides for Staging and Therapy of Medullary Thyroid Cancer and Other Cholecystokinin-B Receptor-Expressing Malignancies. *Seminars in Nuclear Medicine* **2002**, *32*, 97–109.
14. Béhé, M.; Kluge, G.; Becker, W.; Gotthardt, M.; Behr, T.M. Use of Polyglutamic Acids to Reduce Uptake of Radiometal-Labeled Minigastrin in the Kidneys. *J Nucl Med* **2005**, *46*(6), 1012–1015.
15. Breeman, W.A.P.; Fröberg, A.C.; de Blois, E.; van Gameren, A.; Melis, M.; de Jong, M.; Maina, T.; Nock, B.A.; Erion, J.L.; Mäcke, H.R.; et al. Optimised Labeling, Preclinical and Initial Clinical Aspects of CCK-2 Receptor-Targeting with 3 Radiolabeled Peptides. *Nucl. Med. Biol.* **2008**, *35*, 839–849.
16. Good, S.; Walter, M.A.; Waser, B.; Wang, X.; Müller-Brand, J.; Béhé, M.; Reubi, J.-C.; Maecke, H.R. Macroyclic Chelator-Coupled Gastrin-Based Radiopharmaceuticals for Targeting of Gastrin Receptor-Expressing Tumours. *Eur J Nucl Med Mol Imaging* **2008**, *35*, 1868–1877.
17. Klingler, M.; Summer, D.; Rangger, C.; Haubner, R.; Foster, J.; Sosabowski, J.; Decristoforo, C.; Virgolini, I.; von Guggenberg, E. DOTA-MGS5, a New Cholecystokinin-2 Receptor-Targeting Peptide Analog with an Optimized Targeting Profile for Theranostic Use. *J Nucl Med* **2019**, *60*, 1010–1016.
18. Klingler, M.; Hörmann, A.A.; Rangger, C.; Desrues, L.; Castel, H.; Gandolfo, P.; von Guggenberg, E. Stabilization Strategies for Linear Minigastrin Analogues: Further Improvements via the Inclusion of Proline into the Peptide Sequence. *J Med Chem* **2020**, *63*, 14668–14679.
19. Rottenburger, C.; Nicolas, G.P.; McDougall, L.; Kaul, F.; Cachovan, M.; Vija, A.H.; Schibli, R.; Geistlich, S.; Schumann, A.; Rau, T.; et al. Cholecystokinin 2 Receptor Agonist ¹⁷⁷Lu-PP-F11N for Radionuclide Therapy of Medullary Thyroid Carcinoma: Results of the Lumed Phase 0a Study. *J Nucl Med* **2020**, *61*, 520–526.

20. Dorbes, S.; Mestre-Voegtlé, B.; Coulais, Y.; Picard, C.; Silvente-Poirot, S.; Poirot, M.; Benoist, E. Synthesis, Characterization and in Vitro Evaluation of New Oxothenium- and Oxotechnetium-CCK4 Derivatives as Molecular Imaging Agents for CCK2-Receptor Targeting. *Eur. J. Med. Chem.* **2010**, *45*, 423–429.

21. Brillouet, S.; Dorbes, S.; Courbon, F.; Picard, C.; Delord, J.P.; Benoist, E.; Poirot, M.; Mestre-Voegtlé, B.; Silvente-Poirot, S. Development of a New Radioligand for Cholecystokinin Receptor Subtype 2 Scintigraphy: From Molecular Modeling to in Vivo Evaluation. *Bioorg. Med. Chem.* **2010**, *18*, 5400–5412.

22. Scemama, J.L.; Fourmy, D.; Zahidi, A.; Pradayrol, L.; Susini, C.; Ribet, A. Characterisation of Gastrin Receptors on a Rat Pancreatic Acinar Cell Line (AR42J). A Possible Model for Studying Gastrin Mediated Cell Growth and Proliferation. *Gut* **1987**, *28*, 233–236.

23. Aloj, L.; Caraco, C.; Panico, M.; Zannetti, A.; Vecchio, S.D.; Tesauro, D.; Luca, S.D.; Arra, C.; Pedone, C.; Morelli, G.; et al. In Vitro and In Vivo Evaluation of ^{111}In -DTPA-Glu-G-CCK8 for Cholecystokinin-B Receptor Imaging. *J Nucl Med* **2004**, *45*(3), 485–494.

24. Hörmann, A.A.; Klingler, M.; Rezaeianpour, M.; Hörmann, N.; Gust, R.; Shahhosseini, S.; Guggenberg, E. von Initial In Vitro and In Vivo Evaluation of a Novel CCK2R Targeting Peptide Analog Labeled with Lutetium-177. *Molecules* **2020**, *25*, 4585.

25. Fani, M.; Weingaertner, V.; Kolenc Peitl, P.; Mansi, R.; Gaonkar, R.H.; Garnuszek, P.; Mikolajczak, R.; Novak, D.; Simoncic, U.; Hubalewska-Dydyczzyk, A.; et al. Selection of the First $^{99\text{m}}\text{Tc}$ -Labelled Somatostatin Receptor Subtype 2 Antagonist for Clinical Translation-Preclinical Assessment of Two Optimized Candidates. *Pharmaceuticals (Basel)* **2020**, *14*, 19.

26. von Guggenberg, E.; Rangger, C.; Sosabowski, J.; Laverman, P.; Reubi, J.-C.; Virgolini, I.J.; Decristoforo, C. Preclinical Evaluation of Radiolabeled DOTA-Derivatized Cyclic Minigastrin Analogs for Targeting Cholecystokinin Receptor Expressing Malignancies. *Mol Imaging Biol* **2012**, *14*, 366–375.

27. von Guggenberg, E.; Sallegger, W.; Helbok, A.; Ocak, M.; King, R.; Mather, S.J.; Decristoforo, C. Cyclic Minigastrin Analogues for Gastrin Receptor Scintigraphy with Technetium-99m: Preclinical Evaluation. *J. Med. Chem.* **2009**, *52*, 4786–4793.

28. Sauter, A.W.; Mansi, R.; Hassiepen, U.; Muller, L.; Panigada, T.; Wiehr, S.; Wild, A.-M.; Geistlich, S.; Béhé, M.; Rottenburger, C.; et al. Targeting of the Cholecystokinin-2 Receptor with the Minigastrin Analog ^{177}Lu -DOTA-PP-F11N: Does the Use of Protease Inhibitors Further Improve In Vivo Distribution? *J Nucl Med* **2019**, *60*, 393–399.

29. Sosabowski, J.K.; Matzow, T.; Foster, J.M.; Finucane, C.; Ellison, D.; Watson, S.A.; Mather, S.J. Targeting of CCK-2 Receptor-Expressing Tumors Using a Radiolabeled Divalent Gastrin Peptide. *J Nucl Med* **2009**, *50*, 2082–2089.

30. Kolenc-Peitl, P.; Mansi, R.; Tamma, M.; Gmeiner-Stopar, T.; Sollner-Dolenc, M.; Waser, B.; Baum, R.P.; Reubi, J.C.; Maecke, H.R. Highly Improved Metabolic Stability and Pharmacokinetics of Indium-111-DOTA-Gastrin Conjugates for Targeting of the Gastrin Receptor. *J. Med. Chem.* **2011**, *54*, 2602–2609.

31. Ocak, M.; Helbok, A.; von Guggenberg, E.; Ozsoy, Y.; Kabasakal, L.; Kremser, L.; Decristoforo, C. Influence of Biological Assay Conditions on Stability Assessment of Radiometal-Labelled Peptides Exemplified Using a ^{177}Lu -DOTA-Minigastrin Derivative. *Nucl. Med. Biol.* **2011**, *38*, 171–179.

32. Konijnenberg, M.W.; Breeman, W.A.P.; de Blois, E.; Chan, H.S.; Boerman, O.C.; Laverman, P.; Kolenc-Peitl, P.; Melis, M.; de Jong, M. Therapeutic Application of CCK2R-Targeting PP-F11: Influence of Particle Range, Activity and Peptide Amount. *EJNMMI Res* **2014**, *4*, 47.

33. Oberdiac, P.; Mineur, L. Normal tissue tolerance to external beam radiation therapy: The stomach. *Cancer Radiother* **2010**, *14*, 336–339.